ELSEVIER

Polymer 41 (2000) 579–594

polymer

Molecular transport of aromatic solvents in isotactic polypropylene/acrylonitrile-co-butadiene rubber blends

S. George[a], K.T. Varughese[b], S. Thomas[a,*]

[a]*School of Chemical Sciences, Mahatma Gandhi University, Priyadarshini Hills P.O., Kottayam, Kerala 686 560, India*
[b]*Polymer Laboratory, Central Power Research Institute, Bangalore 560 094, India*

Received 28 October 1998; received in revised form 15 February 1999; accepted 12 March 1999

Abstract

The sorption and diffusion of a series of aromatic hydrocarbons through blends of isotactic polypropylene/nitrile rubber have been investigated. The effects of blend ratio, vulcanizing systems and different fillers on the transport behavior were studied. In the blends, the uptake and diffusion coefficient increase with an increase in rubber concentration, and decrease with the molar volume of solvents. The diffusion data were analyzed and it has been observed that most of the systems follow a Fickian mode of transport. The effect of temperature on the transport behavior was investigated at four temperatures. The activation energy for the diffusion, and the thermodynamic parameters like entropy and enthalpy were calculated. The experimental diffusion data were correlated with various theoretical predictions.

Keywords: Blends; Polypropylene; Acrylonitrile-co-butadiene rubber

1. Introduction

During the last few decades the importance of polymer blends have increased, since it is possible to achieve desirable properties by simple blending of polymers. Among the different types of polymer blends thermoplastic elastomers have their own advantages as they combine the processability of plastics with the performance of vulcanized rubbers [1,2]. The possibility of developing new thermoplastic elastomers like polypropylene (PP)/natural rubber (NR), PP/poly(ethylene-co-vinyl acetate) (EVA), PP/ethylene propylene diene rubber (EPDM), high density polyethylene (HDPE)/NR, HDPE/NBR, nylon/EPDM, etc. has been investigated by various researchers [3–7]. However, many of these polymer blends are incompatible or immiscible and are characterized by narrow interface and weak interfacial interaction. They often exhibit poor mechanical properties [8]. These problems associated with immiscible polymer blends could be alleviated by using different techniques like compatibilization and dynamic vulcanization [9–11].

The transport behavior of various organic solvents and gases through polymers is of great technological importance, since nowadays the polymer membranes are increasingly used in various barrier applications [12]. Nitrile rubber, which is an oil resistant elastomer, is widely used in many applications like oil seals, gaskets, etc. For the last few decades, the improvement of the performance of the nitrile rubber has been tried by blending with various polymers [13–16]. The blending of NBR with polypropylene was found to improve the physical and mechanical properties of NBR [17,18]. Hence it is necessary to analyze the transport behavior and the mechanism of transport of various organic solvents through PP/NBR blends in detail.

The transport of small molecules through polymers has been widely studied by various research groups [19–27]. It was found that the transport of the solvents through polymers is influenced by the physical and chemical structure of polymers, the crosslink density, the shape and size of solvent molecules and temperature. The effect of various fillers on the transport behavior of rubbery polymers was investigated [28–30], and it was observed that the presence of fillers makes a tortuous path to the transport of solvents through polymer samples and thereby reduces the solvent uptake. However, the transport behavior is also affected by the interaction of filler between the polymer and the solvent [30].

With the increasing importance of polymer blends in the transport behavior of organic solvents and gases, studies have been directed at polymer blends as well [31–34]. In polymer blends, the transport behavior depends on the miscibility of the component polymers as well as the morphology of the system [31]. Hence the transport

* Corresponding author. Fax: +91-481-561190.

0032-3861/00/$ - see front matter
PII: S0032-3861(99)00208-6

Table 1
Formulation of dynamically vulcanized blends

Sample	$P_{70}S$	$P_{50}S$	$P_{50}C$	$P_{50}M$	$P_{30}S$	P_0S
PP	70	50	50	50	30	–
NBR	30	50	50	50	70	100
ZnO	5	5	–	5	5	5
Stearic acid	2	2	–	2	2	2
Sulfur	0.2	0.2	–	0.1	0.2	0.2
TMTD[a]	2.5	2.5	–	2.5	2.5	2.5
CBS[b]	2	2	–	2	2	2
DCP[c]	–	–	2	1	–	–

[a] Tetramethyl thiuram disulfide.
[b] *N*-cyclohexyl benzothiazyl sulfenamide.
[c] Dicumyl peroxide.

phenomena in polymer blends can be used as a characterization technique, i.e. in order to understand the miscibility as well as morphology of the system. In this paper we have investigated the transport of a series of aromatic solvents through PP/NBR blends. The effects of blend ratio, type of crosslinking and different fillers on the transport phenomena have been studied. The experimental results have been compared with theoretical predictions.

2. Experimental

2.1. Materials

Isotactic polypropylene having an MFI of 3 g/10 min was supplied by IPCL, Baroda. Acrylonitrile-co-butadiene rubber (NBR) with an acrylonitrile content of 34% was purchased from Synthetics and Chemicals, Bareli, U.P. The solvents benzene, toluene and xylene were of analytical grade. The fillers used were HAF-black cork and silica treated with silane coupling agent. The blends were prepared in a Brabender plasticorder by melt mixing at 180° C. The binary blends are denoted as P_{100}, P_{70}, P_{50}, P_{30}, P_0, where the subscripts denote the wt% of NBR in the blend. The formulation of dynamic vulcanized blends is shown in Table 1. In filled blends the filler loading of 30 phr is used and the blends are designated as $P_{50}Tsi_{30}$, $P_{50}C_{30}$ and $P_{50}K_{30}$ respectively for silane treated silica, carbon black and cork filled P_{50} blends.

Samples for transport studies were prepared by compression molding the sample in a hydraulic press into 2 mm thick sheets at 180°C. The circular shaped samples were punched out from the sheet using a sharp edged die.

2.2. Sorption experiments

The samples were soaked in 20 ml solvent in diffusion bottles and kept at constant temperature by keeping in a thermostatically controlled heating oven. The weight of the swollen samples was measured at frequent intervals until equilibrium swelling is reached. The experiments were conducted at 30, 40, 50 and 65°C. A possible source of error in these measurements is that arising during weighing since the sample has to be taken out from the solvent for weighing. However, since the weighing is completed within 20–30 s, the error can be neglected [30]. The results of diffusion experiments were expressed as moles of solvent uptake by 100 g of polymer sample, Q_t mol%.

$$Q_t\text{mol\%} = \frac{\left(\dfrac{\text{Mass of solvent sorbed}}{\text{Molar mass of solvent}}\right)}{\text{Mass of polymer}} \times 100 \quad (1)$$

3. Results and discussion

3.1. Effect of blend ratio

The transport behaviors of unvulcanized and dynamic vulcanized thermoplastic elastomers from PP and NBR were analyzed. The results of the analysis of diffusion experiments of the unvulcanized and vulcanized blends in toluene are shown in Fig. 1(a) and (b), respectively, as mol% uptake (Q_t) vs. square root of time. Polypropylene has the minimum uptake of toluene while NBR has the maximum level. The blends show an intermediate behavior, i.e. between that of the pure components. The lowest value of mol% uptake for polypropylene in spite of the match in solubility parameter between PP and toluene, is due to the crystallinity of PP (Table 2). In a semicrystalline polymer, some amorphous part is also present along with crystalline regions. Only this amorphous region will contribute to the uptake of solvent and hence PP has the lowest uptake value among all the proportions of the blend. In the case of blends, as the concentration of NBR increases, the crystalline content decreases. Hence the hindrance for the transport of toluene decreases and uptake increases. In the blends the crystalline PP phase makes a tortuous path to the transport of solvent through the amorphous regions in blends. Fig. 2 shows the variation of Q_∞ of PP/NBR blends with blend composition. As the concentration of NBR increases, the Q_∞ value increases linearly up to 50 wt% NBR after which a change in slope of the curve is observed. This difference in Q_∞ values with blend composition can be correlated with the morphology of the system. The scanning electron micrographs of P_{70}, P_{50} and P_{30} blends are shown in Fig. 3. It is seen that in P_{70} and in P_{50} NBR is dispersed as spheres in the continuous PP matrix. In the P_{30} blend both NBR and PP form continuous phase leading to a co-continuous morphology. Because of the dispersed nature of NBR phase in P_{70}, the continuous PP phase acts as a tortuous path for the diffusion process of solvent and hence the uptake is less. This is schematically shown in Fig. 4. However, as the concentration of NBR increases from 30 to 50 wt%, the size of NBR domains increases which increases the contact between NBR particles and crystallinity of the blends decreases (Table 2). This leads to the high uptake in P_{50} compared to P_{70}. In P_{30}, where NBR forms the continuous

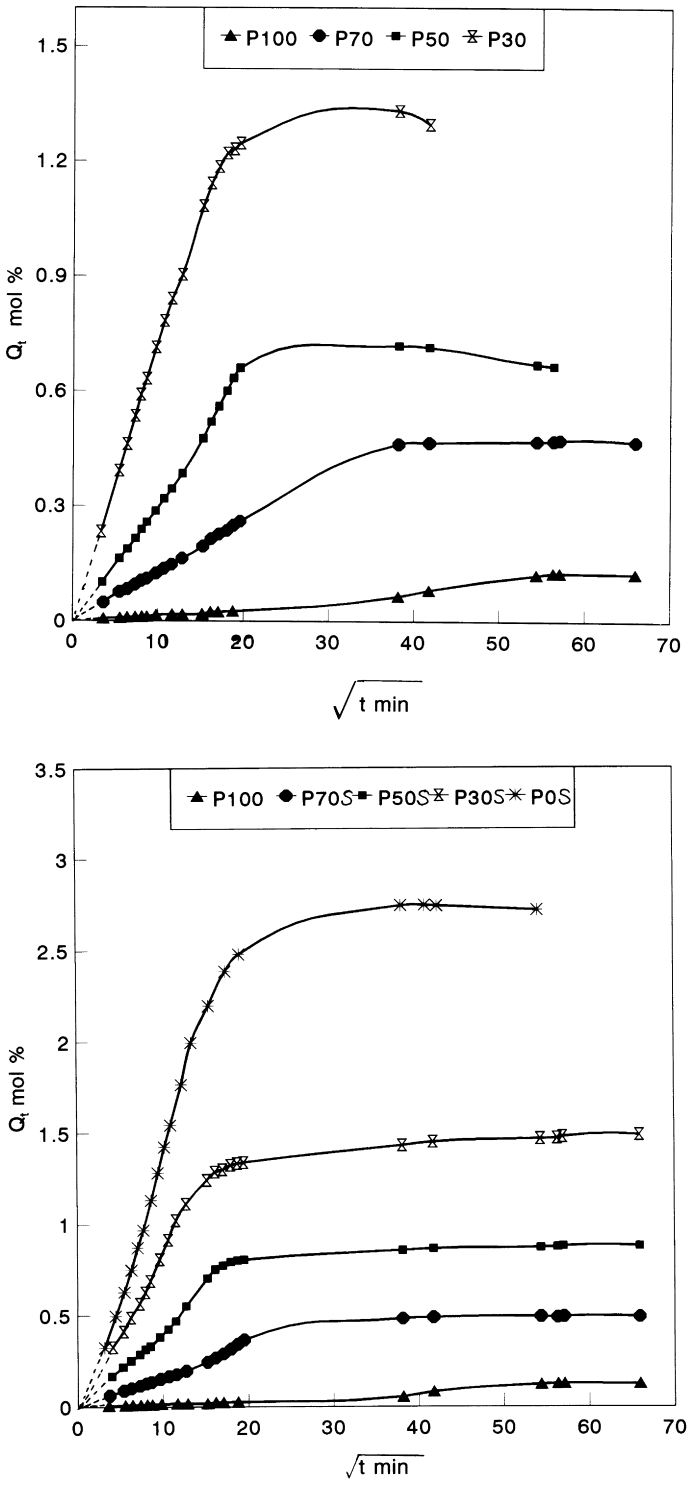

Fig. 1. (a) Variation of mol% toluene uptake (Q_t) with square root of time of unvulcanized PP/NBR blends; (b) variation of mol% toluene uptake (Q_t) with square root of time of dynamically vulcanized PP/NBR blends.

phase the diffusion process is continuous through NBR phase and hence a sharp increase in uptake is observed.

The mechanism of transport of PP/NBR blends was analyzed using the empirical relation [5].

$$\log(Q_t/Q_\infty) = \log k + n\log t \quad (2)$$

where Q_t and Q_∞ are the mol% sorption at time t and at equilibrium, respectively, and k is a constant that depends on the structural characteristics of the polymer and gives information about the interaction between the polymer and solvents. The value of $n = 0.5$ indicates a Fickian mode of transport, while $n = 1$ indicates case II (relaxation

Table 2
Solubility parameter difference and crystallinity of PP/NBR blends

Sample	Solubility parameter difference between polymer and solvent $(cal/cm^3)^{1/2}$	% Crystallinity (from DSC data)
P_{100}	0.20	55.30
P_{70}	0.12	33.90
P_{50}	0.34	20.90
P_{30}	0.56	13.70
P_0	0.88	–

controlled) transport. The value of n between 0.5 and 1 indicates an anomalous transport behavior. The values of n and k for PP/NBR blends are obtained by regression analysis of $\log(Q_t/Q_\infty)$ vs. $\log t$ plot. The results of the analysis are given in Table 3. Since the values range between 0.46 and 0.6, i.e. in PP/NBR blends, the mode of transport is close to Fickian. From the table it is seen that as the concentration of NBR increases the values of n slightly increase and approach the Fickian mode. For the Fickian mode of transport, the rate of diffusion of permeant molecules is much less than the relaxation rate of the polymer chains. Usually rubbers and semicrystalline polymers exhibit Fickian mode of diffusion [31].

The transport of small molecules through polymers generally occurs through a solution diffusion mechanism, i.e. the penetrant molecules are first sorbed by the polymer followed by diffusion through the polymer. The net diffusion through polymer depends on the difference in the amount of penetrant molecules between the two surfaces.

Hence, the permeability [19]

$$P = D \times S \tag{3}$$

where D is the diffusivity and S, the solubility, and the values of S are taken as grams of liquid sorbed per gram of rubber.

The kinetic parameter, the diffusion coefficient D can be calculated using the equation [19,26],

$$\frac{Q_t}{Q_\infty} = 1 - \sum_{n=0}^{\infty}\left[\frac{8}{(2n+1)^2\pi^2}\right] e^{-(2n+1)^2\pi^2(Dt/h^2)} \tag{4}$$

where t is the time and h is the initial thickness of the polymer sheet. Although this equation can be solved readily, it is instructive to examine the short-time limiting expression as well.

$$\frac{Q_t}{Q_\infty} = [4/\pi^{1/2}][Dt/h^2]^{1/2} \tag{5}$$

From a plot of Q_t vs. $t^{1/2}$, a single master curve is obtained which is initially linear. Thus D can be calculated from a rearrangement of Eq. (5) as

$$D = \pi\left(\frac{h\theta}{4Q_\infty}\right)^2 \tag{6}$$

where h is the sample thickness, and θ is the slope of the

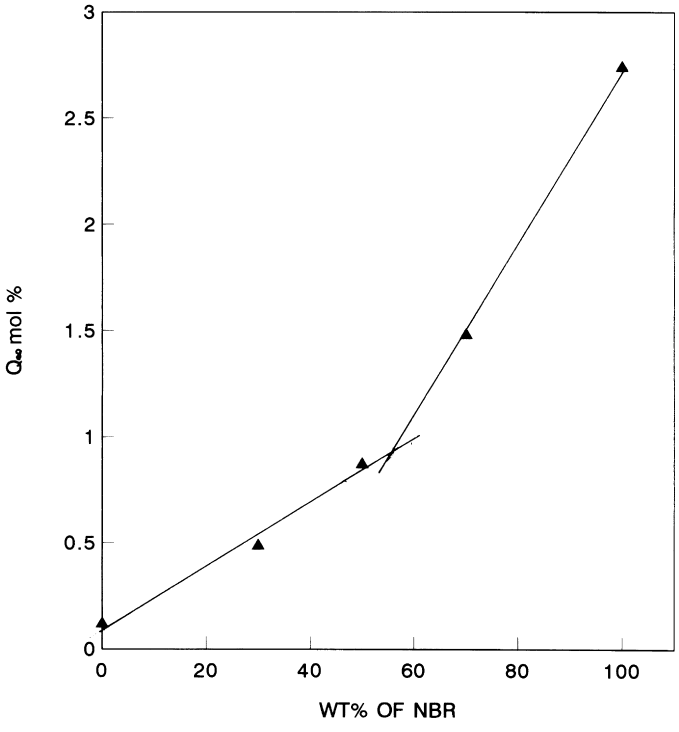

Fig. 2. Variation of equilibrium uptake (Q_∞) of PP/NBR blends with weight percentage of NBR.

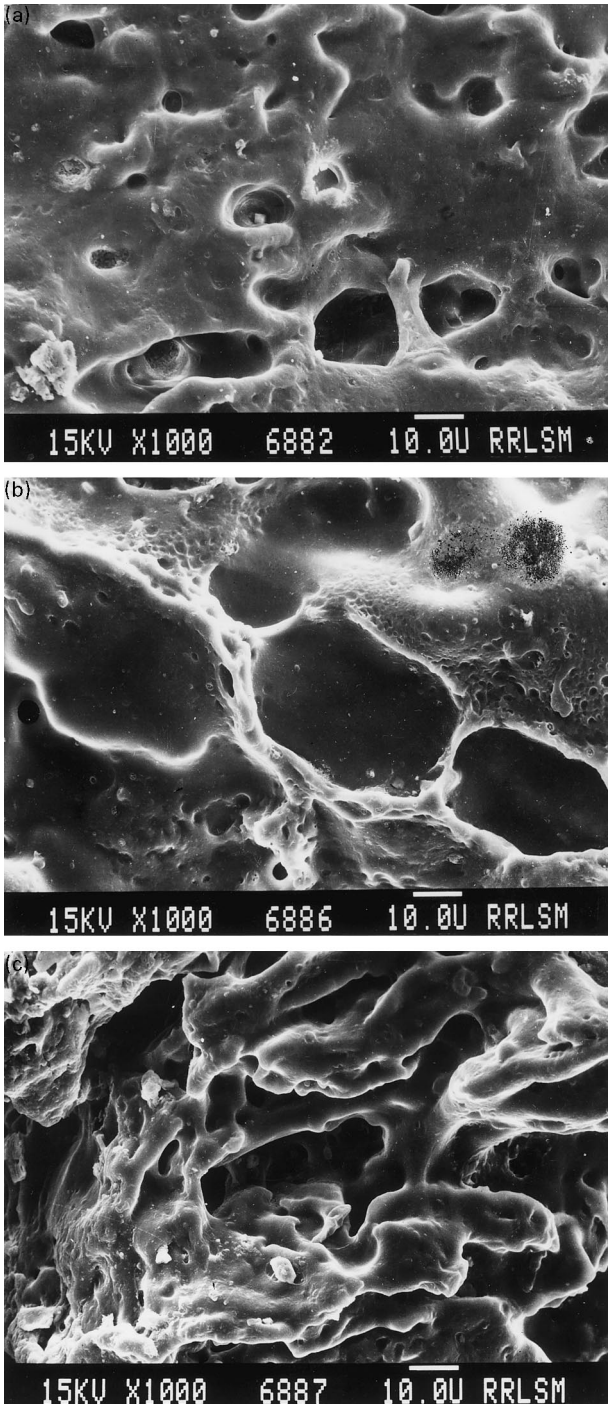

Fig. 3. SEM micrographs of PP/NBR blends: (a) 70/30; (b) 50/50 and; (c) 30/70 PP/NBR blends.

initial linear portion of sorption curves, i.e. before the attainment of 50% of equilibrium uptake. The variation of diffusion and permeation coefficients with blend composition for PP/NBR blends is shown in Fig. 5. It is seen from the figure that PP shows the lowest value for diffusion and permeation coefficient and NBR shows the highest. The blends take intermediate values. As the concentration of NBR increases, the D and P values increase. The increase in D and P values with increase in rubber content is due to the increase in concentration of NBR with a high diffusion coefficient and also due to the fact that the tortuosity exhibited by PP to the penetration of solvent molecules decreases with an increase in NBR content. The change in P and D with rubber content is small up to 50 wt% NBR, after which a sharp increase is observed in these values. This sharp change in the values is due to the phase inversion of NBR from dispersed to continuous phase on passing from 50 to 70 wt% NBR, which leads to an increased diffusion process.

In the case of heterogeneous polymer blends, the permeability can be interpreted in terms of various theoretical models. Robeson's two limiting models, namely series and parallel models, are generally used in the case of polymer blends.

According to the parallel model

$$P_c = P_1\phi_1 + P_2\phi_2 \tag{7}$$

and by the series model

$$P_c = P_1P_2/(\phi_1P_2 + \phi_2P_1) \tag{8}$$

where P_c, P_1 and P_2 are the permeation coefficients of the blend, component I and component II, respectively, and ϕ_1 and ϕ_2 are the volume fractions of components I and II, respectively.

Further, for a conducting spherical filler, the overall composite permeation coefficient is given by Maxwell's equations as [31,35]

$$\overline{P}_c = P_m\frac{P_d + 2P_m - 2\phi_d(P_m - P_d)}{P_d + 2P_m + \phi_d(P_m - P_d)} \tag{9}$$

where the subscripts d and m correspond to the dispersed phase and the matrix, respectively.

Robeson [35] extended Maxwell's analysis to include the continuous and discontinuous characteristics of both phases at intermediate compositions and expressed the equations as:

$$\overline{P}_c = X_a\overline{P}_1\left[\frac{\overline{P}_2 + 2\overline{P}_1 - 2\phi_2(\overline{P}_1 - \overline{P}_2)}{\overline{P}_2 + 2\overline{P}_1 + \phi_2(\overline{P}_1 - \overline{P}_2)}\right] + X_b\overline{P}_2\left[\frac{\overline{P}_1 + 2\overline{P}_2 - 2\phi_1(\overline{P}_2 - \overline{P}_1)}{\overline{P}_1 + 2\overline{P}_{21} + \phi_1(\overline{P}_2 - \overline{P}_1)}\right] \tag{10}$$

where X_a and X_b are the fractional contributions to the continuous phase so that $X_a + X_b = 1$.

Fig. 6 shows the various theoretical and experimental curves showing the variation of P with NBR volume fraction. The P values of PP/NBR blends show an intermediate behavior in between the two limiting models, parallel and series. The experimental data are close to the Maxwell model with PP phase continuous at 70 wt% PP, and at 30 wt% PP the data is close to the Maxwell model with the NBR phase continuous. It is seen from the figure that the experimental curve coincides with Robeson's model for a co-continuous morphology at $X_a = 0.6$ and this suggests that a phase inversion occurs for NBR at this volume

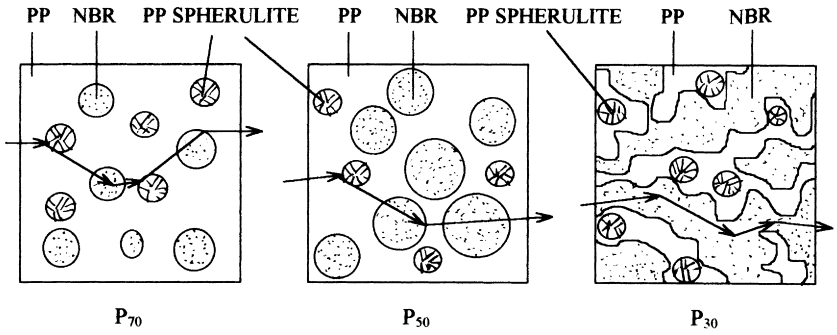

Fig. 4. Schematic representation of the tortuous path exhibited by the crystalline PP phase to the transport of solvent.

fraction. This result is consistent with our early observation from SEM micrographs that phase inversion occurs between 50 and 70 wt% of NBR in the blend.

3.2. Effect of type of crosslinking

The physical and mechanical properties of polymers are found to depend on the nature of crosslinking viz., sulfur or peroxide curing system. In this paper we have investigated the effect of three different crosslinking systems, sulfur, peroxide and a mixed system comprising sulfur and peroxide, on diffusion. Fig. 7 shows the Q_t vs. $t^{1/2}$ curves of dynamically vulcanized P_{50} blends. Among the different vulcanizing systems used, the DCP crosslinked system shows the lowest uptake. Sulfur cured system shows the highest solvent uptake and the mixed system takes an intermediate position. The values of D, P, n and k for these samples are given in Table 4. It is seen from the table that the values of n vary from 0.46 to 0.052 for the three systems, i.e. sulfur system shows the lowest n value while the DCP system shows the highest. All the three systems follow an almost Fickian mode of transport. When we examine the k values it is seen that the DCP crosslinked systems show the lowest k value and sulfur and mixed crosslinked systems show almost similar values which is higher than that of the DCP system. Hence the interaction between solvent and polymer blend is low for DCP crosslinks compared to sulfur and mixed systems. The diffusion and permeation coefficients of toluene are low in the case of DCP compared to sulfur and mixed systems. The difference in the transport parameters of these three different vulcanizing systems arises from the type of crosslinks formed and also due to the extent of crosslinking, i.e. the crosslink density. Among the three vulcanizing systems used, sulfur vulcanization leads to the formation of S–S linkages while DCP vulcanization gives rise to rigid C–C linkages. In mixed systems, both types of crosslinks are present (Fig. 8). Since in the DCP system the diffusion of solvents is more difficult due to the rigid nature of C–C linkages, it shows the lowest uptake and low diffusion coefficient values. The presence of more flexible S–S linkages permits the solvents to permeate more easily through the sulfur vulcanized samples and hence they show the highest uptake. In mixed vulcanized system, an intermediate behavior is expected, since it contains both C–C and S–S linkages. But the results indicate that the mixed system shows almost the same behavior as that of the sulfur system. This can be explained using crosslink density and molar mass between the crosslinks for the different vulcanizing systems.

Table 3
n and k values for diffusion of toluene through PP/NBR blends

Sample	n	k (g/g min^n)
P_{100}	0.46	0.01
$P_{70}S$	0.47	0.04
$P_{50}S$	0.47	0.05
$P_{30}S$	0.51	0.05
P_0S	0.60	0.03

The molar mass between crosslinks (M_c) of the network polymer chain was calculated using the relation developed by Flory–Rehner [36].

$$M_c = \frac{-\rho_p V_s(\phi^{1/3} - \phi/2)}{\ln(1-\phi) + \phi + \chi\phi^2} \tag{11}$$

where ρ_p is the density of the polymer, V_s, the molar volume of solvent and ϕ, the volume fraction of swollen rubber in the fully swollen sample. The volume fraction of the swollen rubber is estimated by considering PP as a filler in NBR since the uptake of PP is low, which is given by

$$\phi = \frac{(d - fw)\rho_p^{-1}}{(d - fw)\rho_p^{-1} + A_s\rho_s^{-1}} \tag{12}$$

where d is the deswollen weight of the polymer, f the volume fraction of filler; w the initial weight of sample; ρ_p the density of the polymer, ρ_s the density of the solvent and A_s, the weight of the solvent in the swollen sample.

$$\chi = \beta + \frac{V_s(\delta_s - \delta_p)^2}{RT} \tag{13}$$

where β is the lattice constant ($=0.34$), δ the solubility parameter, and V_s the molar volume of the solvent.

The values of M_c and the crosslink density are given in Table 5. It is seen that the M_c values are in the order DCP $<$ mixed $\cong$ sulfur system, i.e. the molar mass between the crosslinks is more in the case of mixed vulcanized system

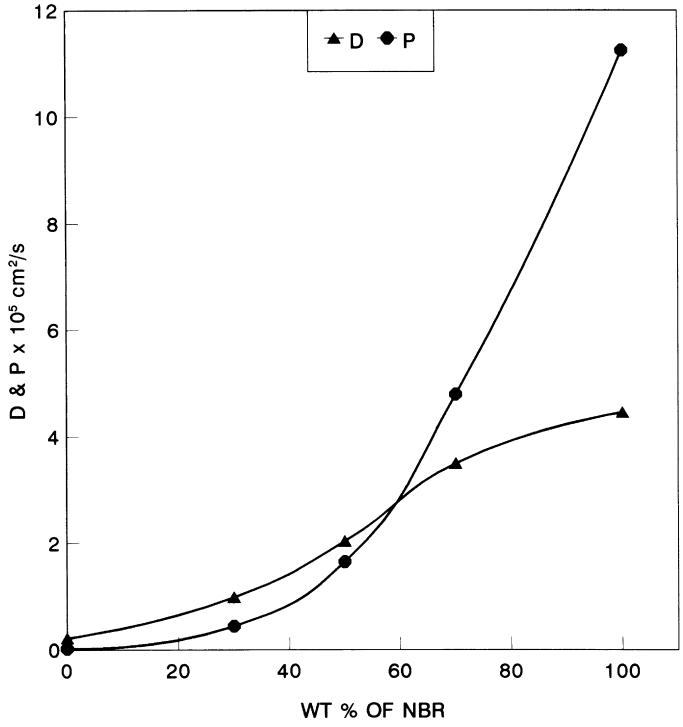

Fig. 5. Variation of diffusion and permeation coefficient with weight percentage of NBR.

and lowest for the DCP system. Since M_c is inversely proportional to crosslink density, the crosslink density follows the order DCP > mixed ≅ sulfur, i.e. the DCP vulcanized system with the highest crosslink density permeates less solvent molecules compared to sulfur and mixed vulcanized systems. Since blends vulcanized with sulfur and mixed system have the same crosslink density, the uptake may be comparable. Hence the combined effect

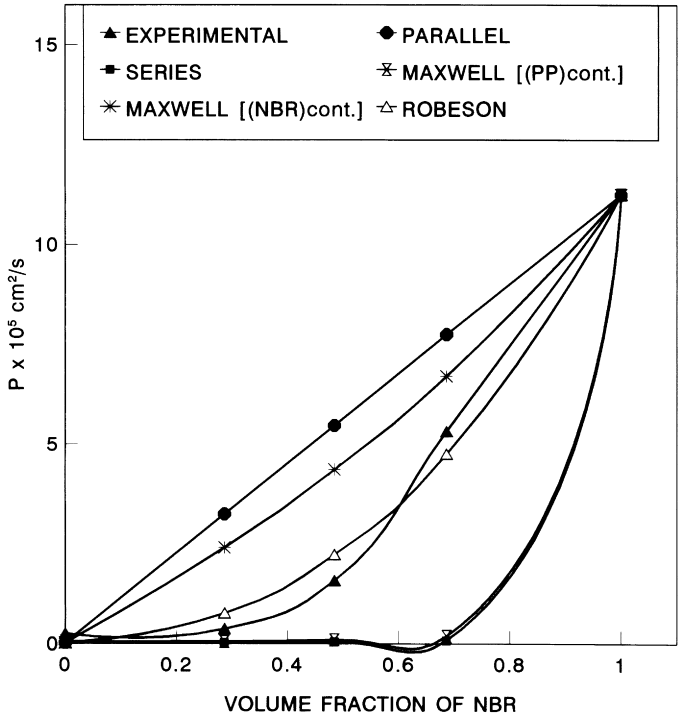

Fig. 6. Experimental and theoretical version of permeation coefficient with volume fraction of NBR is the blends.

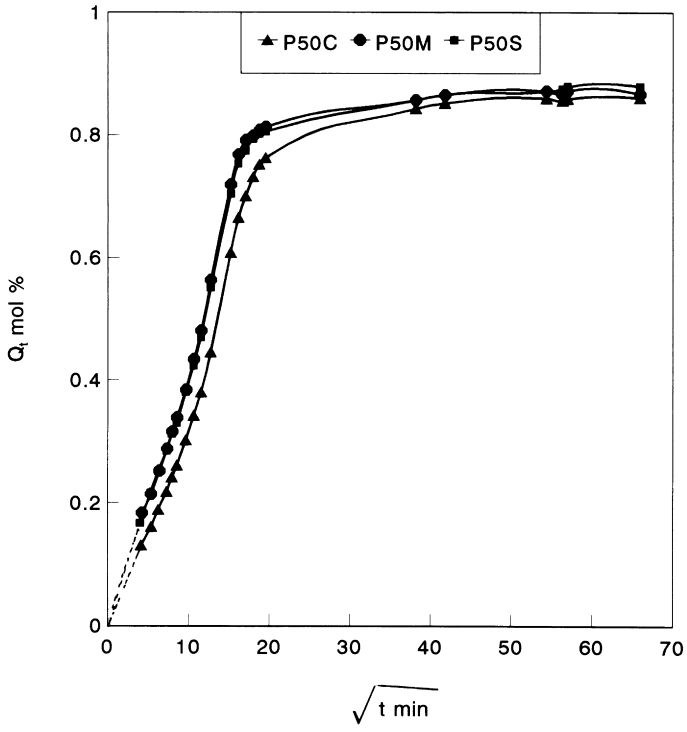

Fig. 7. Variation of mol% uptake of toluene (Q_t) with square root of time for various dynamically crosslinked P_{50} blends.

of the crosslink density and rigidity of bonds accounts for the transport behavior in sulfur and mixed systems.

3.3. Effect of penetrant size

The sorption behavior of organic solvents through polymer samples is affected by the size, shape and polarity of penetrant molecules. Fig. 9 shows the sorption curves of P_{50} blend crosslinked with sulfur for benzene, toluene and xylene. As expected, as the size of penetrant molecules increases the solvent uptake decreases, i.e. the low molecular weight solvent benzene shows the highest uptake and xylene, the high molecular weight solvent shows the lowest uptake. The variation of Q_∞ with molar volume of solvent for different blend compositions is shown in Fig. 10. It is seen that the Q_∞ values decrease linearly with the molar volume of penetrant for all the blend compositions. The rate of decrease in Q_∞ with molar volume increases with increase in concentration of NBR.

The influence of penetrant size on the mechanism of transport, diffusion and permeation coefficients of various

Table 4
Transport parameters for diffusion of toluene through dynamically vulcanized P_{50} blends

Sample	n	k (g/g min^n)	D ($\times 10^5$ cm^2/s)	P ($\times 10^5$ cm^2/s)
P_{50}S	0.46	0.05	2.03	1.64
P_{50}C	0.52	0.03	1.81	1.43
P_{50}M	0.47	0.05	2.22	1.78

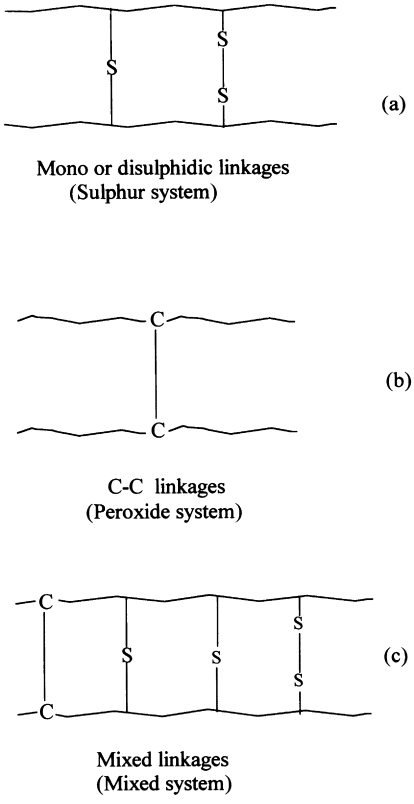

Fig. 8. Schematic representation of the types of crosslinks formed in (a) sulfur; (b) peroxide and; (c) mixed cured P_{50} blends.

Table 5
M_c and crosslink density values of dynamically vulcanized P_{50} blends

Sample	M_c	Crosslink density ($\times 10^{-4}$ g mol/cm^3)
$P_{50}S$	1673.02	5.97
$P_{50}C$	1252.08	7.99
$P_{50}M$	1671.78	5.98

polymer blends was analyzed and the results are given in Table 6. The *n* values decrease with increase in molecular weight of the penetrants. In the case of *k* values, there is no regular trend. However, in general, toluene shows the highest *k* value and hence more interaction with the polymer. Both *D* and *P* values, decrease with the penetrant size for the pure NBR and blends.

3.4. Effect of fillers

The incorporation of filler into polymer networks is found to decrease the sorption and diffusion of solvents. Fig. 11 depicts the sorption curves of unfilled and 30 phr loaded silica, carbon black and cork filled P_{50} blends. It is seen from the figure that the initial uptake of toluene is not much affected by the presence of fillers. However, the equilibrium uptake values are lower for the filled blends compared with unfilled ones. Among the three fillers used, the C-black filled blends showed the lowest equilibrium uptake. The uptake behavior of different blends follows the order $P_{50} > P_{50}K_{30} > P_{50}Tsi_{30} > P_{50}C_{30}$. Table 7 shows the *n*, *k*, *D* and *P* values of these blends. Compared with the unfilled blend the *n* values increase for silica and C-black loaded blends, while in cork filled sample *n* decreases. The *k* values increase upon the incorporation of cork while in the other two cases, the *k* value shows a decrease. While considering the diffusion and permeation coefficients, it is seen that the values are higher than the unfilled blend in the case of C-black and silica-filled samples and lower for the cork-filled blend. The difference in the behavior of the filled blends on the diffusivity and permeability and in the equilibrium values may be related to the interaction between the filler and polymer. It has been reported that in thermoplastic elastomers, the filler particles generally concentrate in the rubber phase. Since silica filler surface is polar, it shows better interaction with the polar NBR particles which may lead to more phase separation, i.e. interaction between PP and NBR decreases, which leads to weak interphases. This weak interphase may enhance the diffusion and permeation of solvents through the membrane which increases the *D* and *P* values. However, the final equilibrium values depend mainly on the extent of crosslink density and reinforcement exerted by the filler.

The extent of reinforcement is assessed by using the Kraus equation [37], according to which

$$V_{r0}/V_{rf} = 1 - m[f/1 - f] \quad (14)$$

where V_{rf} is the volume fraction of swollen rubber in the fully swollen filled sample, *f* is the volume fraction of filler and *m* is a measure of the extent of reinforcement.

The crosslink density and extent of reinforcement (*m*) of different fillers obtained from the Kraus equation for various

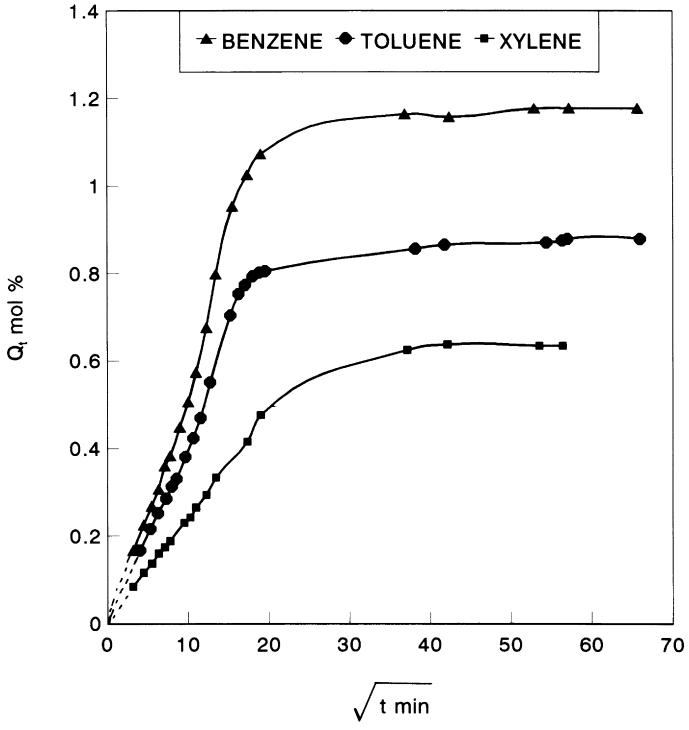

Fig. 9. Variation of mol% uptake (Q_t) with square root of time for the diffusion of benzene, toluene and xylene through P_{50} blends.

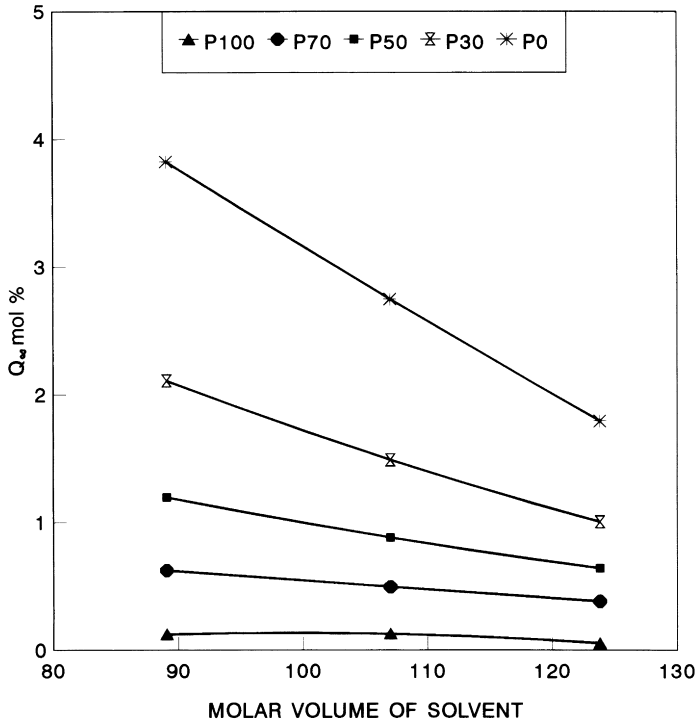

Fig. 10. Variation of equilibrium uptake (Q_∞) of toluene in P_{50} blends with molar volume of solvents.

filled and unfilled blends are shown in Table 8. It is seen that the crosslink density decreases in filled blends as compared with unfilled P_{50} blend. Hence, the reduction in equilibrium uptake in filled blends is due to the reinforcement exerted by the fillers. Among the filled blends, the crosslink density varies in the order $P_{50}C_{30} > P_{50}Tsi_{30} > P_{50}K_{30}$ and the extent of reinforcement follows the order: $P_{50}Tsi_{30} > P_{50}C_{30} > P_{50}K_{30}$. Hence cork-filled P_{50} blend with the lowest crosslink density and reinforcement shows the highest uptake among the filled samples. The C-black filled sample with the highest crosslink density and intermediate reinforcement shows the lowest uptake.

Table 6
Transport parameters for diffusion of various solvents (B = benzene, T = toluene, X = xylene) through PP/NBR blends

		n	k (g/g min^n)	D ($\times 10^5$ cm^2/s)	P($\times 10^5$ cm^2/s)
P_{100}	B	0.05	0.01	0.07	0.01
	T	0.46	0.01	0.22	0.02
	X	0.53	0.01	0.76	0.01
$P_{70}S$	B	0.47	0.04	0.01	0.01
	T	0.47	0.04	0.99	0.45
	X	0.42	0.04	0.58	0.23
$P_{50}S$	B	0.50	0.04	2.26	2.11
	T	0.47	0.05	2.03	1.65
	X	0.48	0.05	1.44	0.98
$P_{30}S$	B	0.51	0.05	3.54	5.53
	T	0.51	0.05	3.50	4.79
	X	0.48	0.05	2.50	2.66
P_0S	B	0.63	0.03	5.53	11.65
	T	0.60	0.03	4.45	11.28
	X	0.58	0.03	3.73	7.08

3.5. Effect of temperature

The effect of temperature on mol% uptake of P_{50} blends is shown in Fig. 12. As the temperature increases, the uptake of solvent increases as expected. The rates of diffusion and permeation also increase with increase in temperature. The temperature dependence of transport properties can be used to evaluate the activation energy for the diffusion and permeation processes using the Arrhenius relation

$$X = X_0 \exp - (E_a/RT) \quad (15)$$

where X is P or D; E_a, the activation energy, R, the universal gas constant; and T, the absolute temperature. The Arrhenius plots of $\log D$ and $\log P$ vs. $1/T$ for different blend compositions are shown in Figs. 13 and 14, respectively. From the Arrhenius plots, the values of activation energy for permeation and diffusion were calculated using regression analysis. The results are shown in Tables 9 and 10. In different blend compositions, the activation energy for diffusion decreases with increase in rubber concentration, while activation energy for permeation did not show a regular trend. Among the different vulcanizing system used, the DCP vulcanized system shows the highest activation energy and mixed system shows the lowest value. The highest activation energy observed in DCP crosslinked system may arise from the rigidity of C–C linkages compared with S–S linkages present in sulfur and mixed systems. It

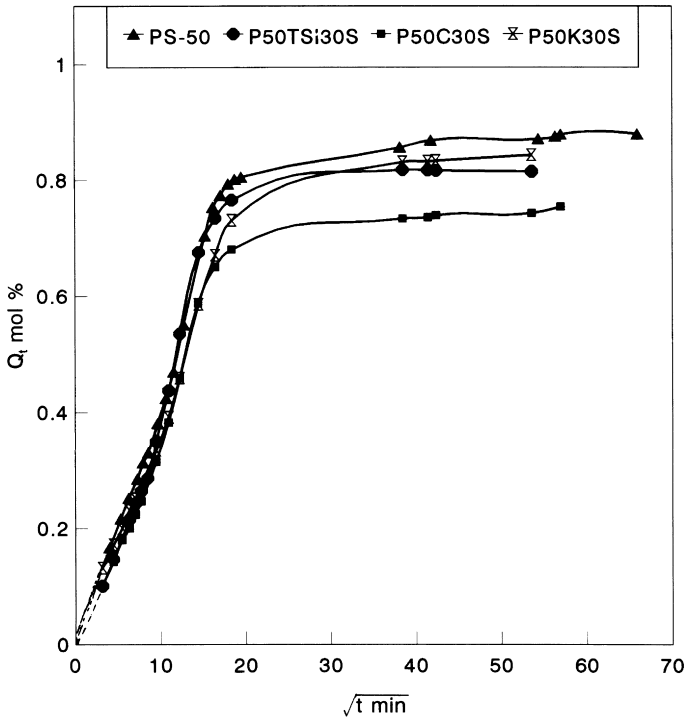

Fig. 11. Variation of mol% uptake of toluene with square root of time for various filled P_{50} blends.

is also interesting to note that the activation energy decreases upon the incorporation of filler. The toluene shows the highest activation energy among the solvents used.

3.6. Thermodynamic parameters

The thermodynamics parameters for diffusion, ΔH and ΔS can be calculated using van't Hoff's relation:

$$\log K_s = \frac{\Delta S^\circ}{2.303R} - \frac{\Delta H^\circ_s}{2.303RT} \quad (16)$$

where K_s is equilibrium sorption constant which is given by

$$K_s = \frac{\text{No. of mols of solvent sorbed at equilibrium}}{\text{Mass of the polymer}}. \quad (17)$$

The values of ΔS and ΔH are obtained by regression analysis of the plots of log K_s vs. $1/T$. The values of ΔH° and ΔS° are given in Table 11. It is seen from the table that the ΔH values are positive and vary from 2.2 to 4.6 kJ/mol. The positive values of ΔH indicate that the sorption is an endothermic process and is dominated by Henry's mode, i.e. the sorption proceeds through creation of new sites or pores in the polymer. In the case of blends with different NBR compositions, the ΔH value decreases with increase in NBR content.

Table 7
Transport parameters for diffusion of toluene through filled P_{50} blends

	n	k (g/g min^n)	D ($\times 10^5$ cm^2/s)	P ($\times 10^5$ cm^2/s)
T-silica	0.56	0.03	2.36	1.78
C-black	0.51	0.04	2.36	1.64
Cork	0.44	0.06	1.93	1.50

3.7. Kinetics of diffusion

The first-order kinetic model has been used to follow the kinetics of sorption and diffusion of solvents through PP/NBR blends. In order to apply this kinetic model it is assumed that during sorption of solvents, structural changes may occur in polymer chains which require a rearrangement of the polymer segments that can dominate the kinetic behavior. According to the first-order kinetic equation,

$$dc/dt = k'(C_\infty - C_t) \quad (18)$$

where k' is the first-order rate constant, and C_t and C_∞ represent the concentrations at time t and at equilibrium, respectively. Integration of the above equation gives

$$k't = 2.303\log[C_\infty/(C_\infty - C_t)] \quad (19)$$

Figs. 15 and 16 show plots of $\log(C_\infty - C_t)$ vs. t for various blend compositions in toluene. From these plots, the first-order rate constants were calculated by regression analysis and the results are given in Table 12. As expected, the rate constant values increase with an increase in concentration of rubber in the blends. Among the vulcanized systems, the DCP vulcanized system shows the lowest k' value, while the mixed system shows the highest value. The sulfur vulcanized blend shows an intermediate behavior. In filled

Table 8
Crosslink density and extent of reinforcement of filled P_{50} blends

	Crosslink density ($\times 10^{-4}$ g mol/cm^3)	m
Unfilled	2.28	
T-silica	1.87	− 1.71
C-black	2.11	− 0.53
Cork	1.35	0.82

Table 9
Activation energy for diffusion and permeation of toluene in PP/NBR blends

	E_P (kJ/mol)	E_D (kJ/mol)
$P_{70}S$	21.54	26.15
$P_{50}S$	20.31	23.66
$P_{30}S$	18.03	29.86
$P_{50}P$	23.48	26.31
$P_{50}M$	12.27	17.04
$P_{50}Tsi_{30}$	19.15	21.29

Table 10
Activation energy for diffusion and permeation of various solvents (B = benzene, T = toluene, X = xylene) in PP/NBR blends

		E_D (kJ/mol)	E_P (kJ/mol)
$P_{50}S$	B	17.95	21.48
	T	20.31	23.66
	X	18.40	21.36
$P_{50}Tsi_{30}$	B	16.90	20.57
	T	19.15	21.29
	X	16.04	18.20

Table 11
Thermodynamic parameters for diffusion of toluene through PP/NBR blends

Sample	$\Delta H°$ (kJ/mol)	$\Delta S°$ (J/mol/deg)	$-\Delta G$
$P_{70}S$	4.60	28.78	4.02
$P_{50}S$	3.16	28.86	5.49
$P_{30}S$	2.77	25.90	4.99
$P_{50}M$	4.70	24.00	2.49
$P_{50}P$	3.71	27.32	4.48
$P_{50}Tsi_{30}$	2.13	32.94	4.48

Table 12
Rate constant values for the transport of toluene in PP/NBR blends

Sample	Rate constant k ($\times 10^3$ min^{-1})
P_{100}	0.22
$P_{70}S$	1.04
$P_{50}S$	1.95
$P_{30}S$	2.80
P_0S	2.66
$P_{50}P$	1.55
$P_{50}M$	2.03
$P_{50}Tsi_{30}$	2.25
$P_{50}K_{30}$	2.19
$P_{50}C_{30}$	2.14

Table 13
Theoretical and experimental M_c values for dynamically vulcanized PP/NBR blends

	M_c		
	Experimental	Affine	Phantom
$P_{70}S$	1196.32	520.40	173.46
$P_{50}S$	1673.02	1283.94	427.98
$P_{50}P$	1252.02	978.94	326.31
$P_{50}M$	1671.78	1282.99	427.66
$P_{30}S$	2992.19	2261.16	753.64

systems, the rate constant values are higher as compared with unfilled systems.

3.8. Comparison with theory

The chemical crosslink density calculated was correlated with those of affine and phantom network models [21]. In the affine network model, it is assumed that the junction points are embedded in the network without fluctuations, so that the components of each chain vector transform linearly with macroscopic deformation.

According to the affine network model, the molecular weight between crosslinks is given by

$$M_c(\text{aff}) = \frac{\rho V_s v_{2c}^{2/3} v_{2m}^{1/3}\left(1 - \frac{\mu}{\nu} v_{2m}^{1/3}\right)}{-(\ln(1 - v_{2m}) + v_{2m} + \chi v_{2m}^2)} \quad (20)$$

where V_s is the molar volume of solvent, μ, the number of effective chains, ν, the number of junctions, v_{2m}, the polymer volume fraction at equilibrium swelling, v_{2c}, the polymer volume fraction during crosslinking, and ρ, the polymer density.

In the case of the phantom network model, the chains can move freely through one another, i.e. the junction points fluctuate over time around their mean position without any hindrance from the neighboring molecules. In the phantom network model, M_c is calculated using the relation

$$M_c(\text{ph}) = \frac{\left(1 - \frac{2}{\phi}\right)\rho V_s v_{2c}^{2/3} v_{2m}^{1/3}}{-(\ln(1 - v_{2m}) + v_{2m} + \chi v_{2m}^2)} \quad (21)$$

where ϕ is the junction functionality.

The results obtained from these calculations are shown in Table 13. From the table it is seen that the experimental values are close to the affine network model. Hence in PP/NBR blends, the crosslinked junctions are embedded in the network, so that they cannot fluctuate freely and the chain vector transforms linearly with macroscopic deformation.

Attempts have been made to compare the experimental diffusion curves with the theoretical diffusion profile. The theoretical curves are constructed using the equation which

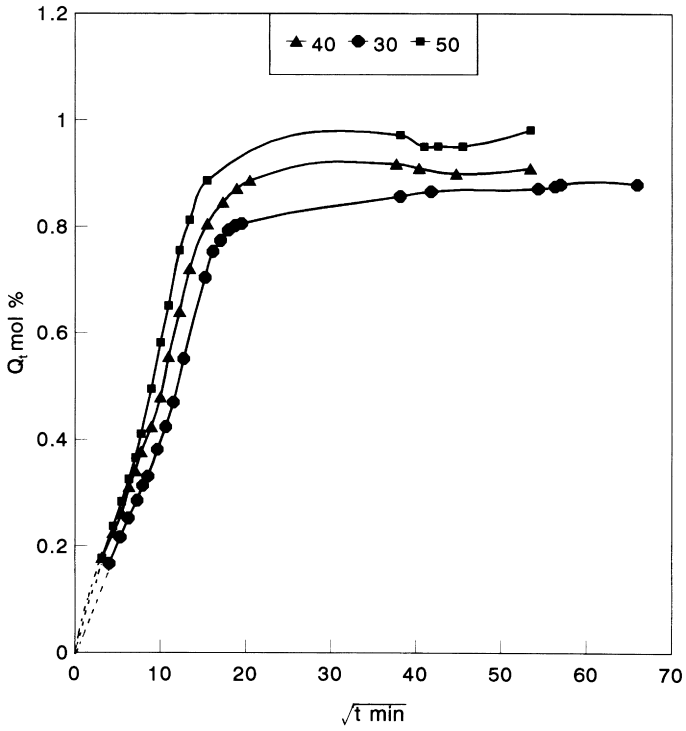

Fig. 12. Variation of mol% uptake (Q_t) of toluene with square root of time at various temperatures.

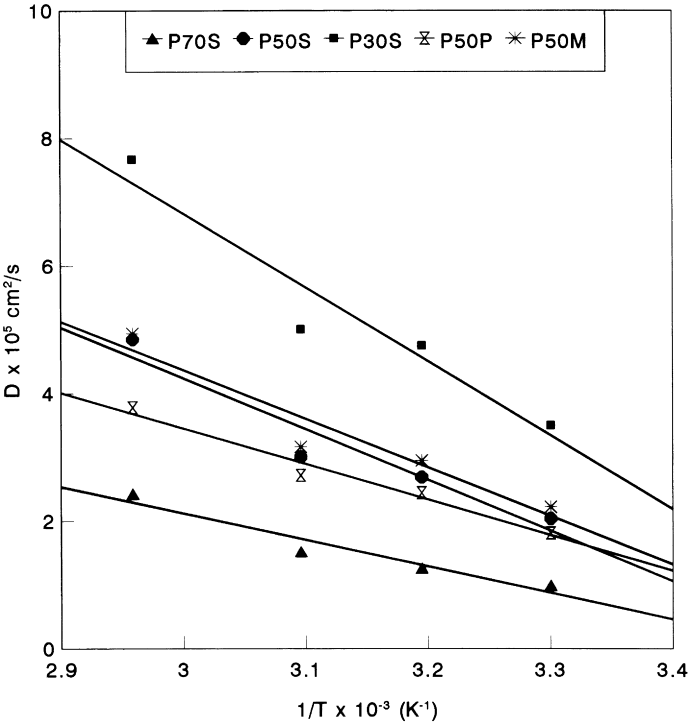

Fig. 13. Arrhenius plots of log D vs. $1/T$ of dynamically vulcanized P_{50} blends.

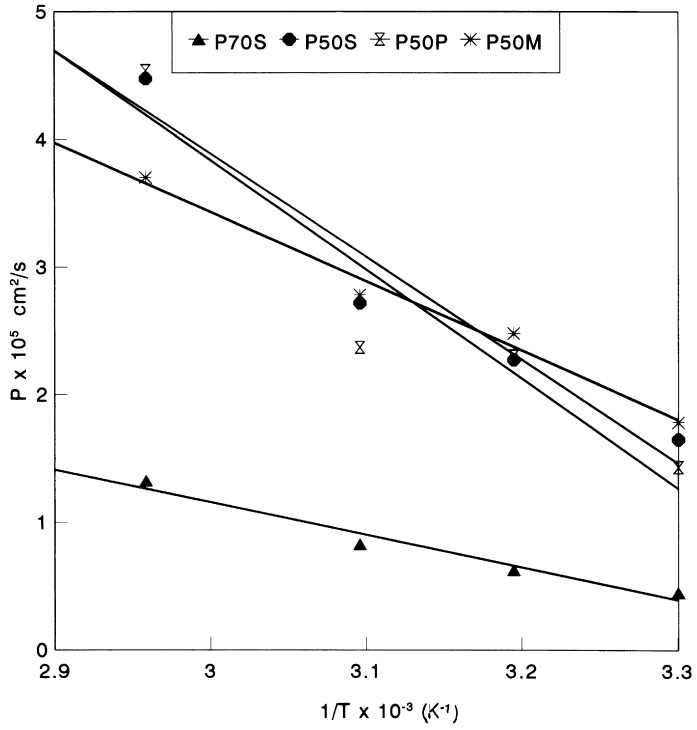

Fig. 14. Arrhenius plots of log P vs. $1/T$ of dynamically vulcanized P_{50} blends.

describes the Fickian diffusion model:

$$\frac{Q_t}{Q_\infty} = 1 - \frac{8}{\pi^2}\sum_{n=0}^{\infty} 1/(2n+1)^2 \exp[-D(2n+1)^2\pi^2 t/h^2]. \quad (22)$$

In order to generate the diffusion curves, the experimentally determined D values are substituted in Eq. (22). Fig. 17 shows the theoretical and experimental sorption curves of P_{70}, P_{50} and P_{30} blends in toluene. The overall agreement between the experimental and theoretical curves is fairly

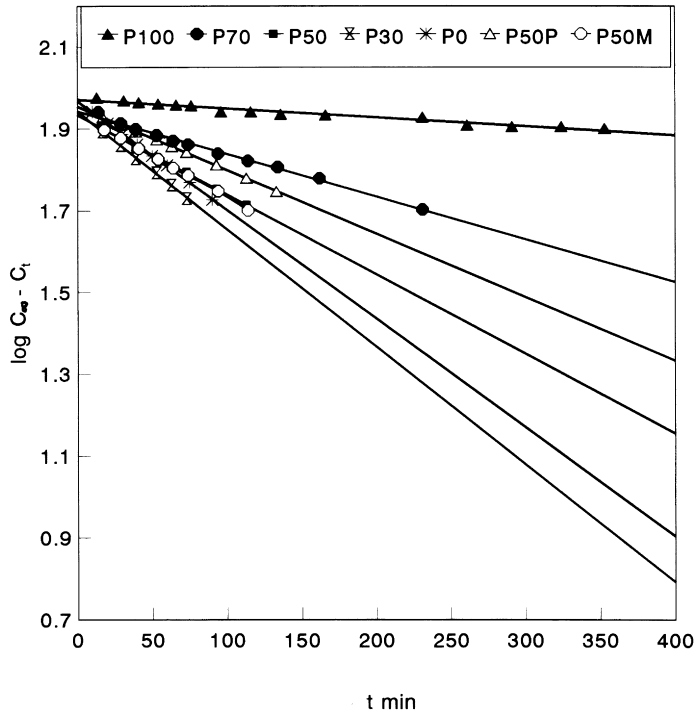

Fig. 15. Variation of $\log(C_\infty - C_t)$ vs. time of PP/NBR blends.

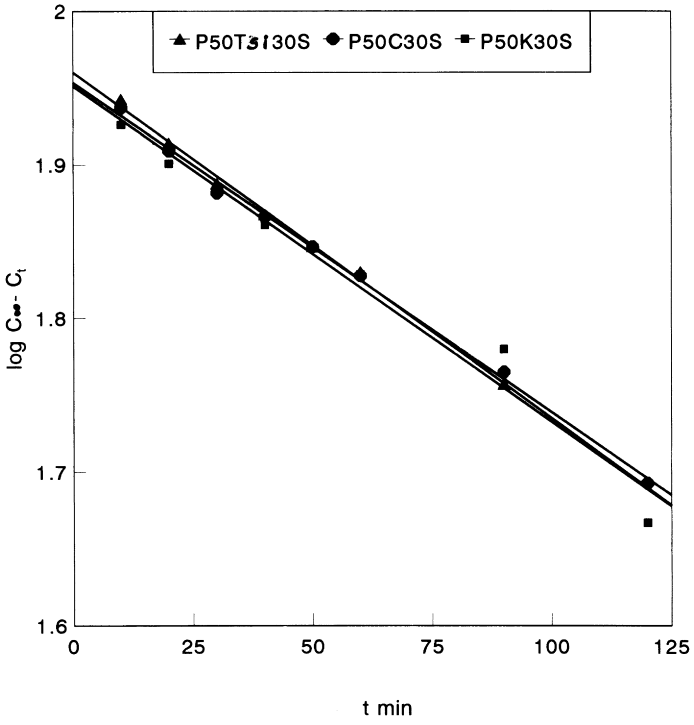

Fig. 16. Variation of $\log(C_\infty - C_t)$ vs. time of filled P_{50} blends.

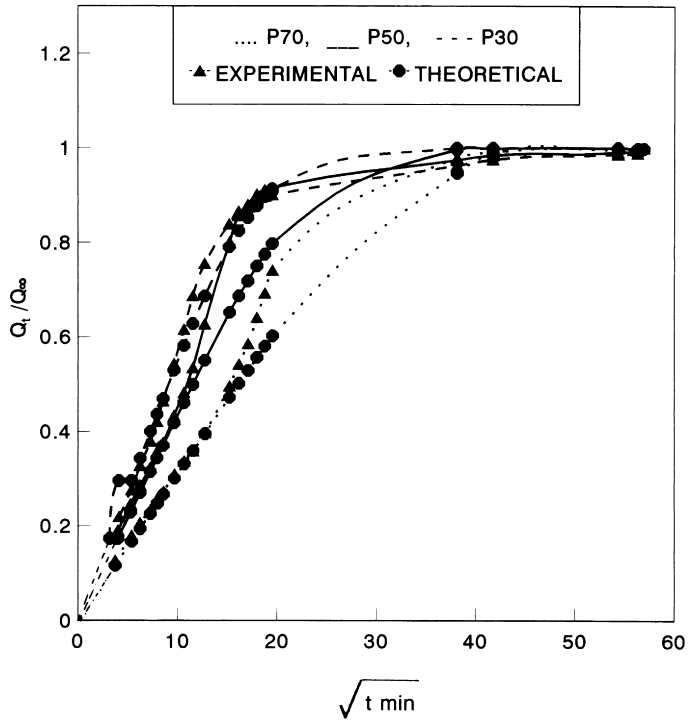

Fig. 17. Experimental and theoretical diffusion curves of P_{70}, P_{50} and P_{30} blends.

good. A similar behavior was observed for other blend systems and solvents as well.

4. Conclusions

The transport behavior of various aromatic solvents through PP/NBR blends was investigated. The transport phenomena follows a Fickian trend in PP/NBR blends. As the concentration of NBR increases in the blend, the equilibrium uptake values and diffusion and permeation coefficients are increased. The variation in transport parameters was correlated with the morphology of the system. The equilibrium uptake values show a sharp increase after 50 wt% NBR which is due to the phase inversion of NBR from dispersed to continuous phase. The experimental permeation coefficients were compared with various theoretical predictions. Maxwell and Robeson's models have been used to predict the experimental permeation coefficients. The effect of type of crosslinking on transport behavior was studied. Among the three vulcanizing systems used (sulfur, DCP and mixed (S + DCP) systems), the sulfur system showed the highest uptake and DCP the lowest and mixed system showed intermediate behavior. The difference in the behavior was correlated with type of crosslinks formed, i.e. S–S, C–C and C–C + S–S linkages and crosslinking density. The diffusion and permeation coefficients and Q_∞ values decreased with increase in molar volume of solvents. The effect of different types of filler on transport properties was also investigated. In the filled blends, the uptake values follows the order cork > silica > carbon black. The activation energy for diffusion and permeation was calculated. The activation energy for diffusion decreases with an increase in rubber concentration. Comparison of the crosslink density values with phantom and affine network models indicates that in PP/NBR blends, the network structure could be modeled by the affine theory. The experimental and theoretical diffusion curves are in good agreement for the blend systems.

Acknowledgements

One of the authors (S.G.) is thankful to the Council of Scientific and Industrial Research, New Delhi, for the financial assistance for this work.

References

[1] De SK, Bhowmick AK, editors. Thermoplastic elastomers from rubber–plastic blends New York, NY: Ellis Horwood, 1990.
[2] Walker BM, editor. Handbook of thermoplastic elastomers New York, NY: Van Nonstrand Reinhold, 1979.
[3] Yoon LK, Choi CH, Kim BY. J Appl Polym Sci 1995;56:239.
[4] Campbell DS, Elliot DJ, Wheelans MA. NR Technol 1978;9:21.
[5] Kuriakose B, De SK. Mater Chem Phys 1985;12:157.
[6] Coran AY, Patel R, Williams D. Rubber Chem Technol 1982;55:116.
[7] Koros WJ, editor. Barrier polymers and structures ACS Symposium Series, 423. Washington, DC: American Chemical Society, 1990.
[8] Paul DR, editor. Polymer blends, II. New York, NY: Academic Press, 1976 Chapter 12.
[9] Thomas S, Prud'homme RE. Polymer 1992;33:4260.
[10] Miettinen RMH, Seppala JV, Ikkala OT, Reima IT. Polym Engng Sci 1994;5:395.
[11] Lia FS, Su AC, Hsu T-C. Polymer 1994;35:2579.
[12] Varughese KT, Nando GB, De PP, De SK. J Mater Sci 1988;23:3894.
[13] Liu NC, Xie HQ, Baker WE. Polymer 1993;34:4680.
[14] George J, Joseph R, Varughese KT, Thomas S. J Appl Polym Sci 1995;57:449.
[15] Coran AY, Patel R. Rubber Chem Technol 1983;56:1045.
[16] George S, Joseph R, Varughese KT, Thomas S. Polymer 1995;36(23):4405.
[17] George S, Neelakantan NR, Varughese KT, Thomas S. J Polym Sci B: Polym Phys 1997;35:2309.
[18] George S, Ramamurthy K, Anand JS, Varughese KT, Thomas S. Submitted to Polymer for publication.
[19] Shivaputrappa B, Harogappad A, Aminabhavi TM. Macromolecules 1991;24:2598.
[20] Schneider NS, Illinger JL, Cleaves MA. Polym Engng Sci 1986;26(22):1547.
[21] Liao DC, Chern YC, Han JL, Hseih KH. J Polym Sci B: Polym Phys 1997;35:1747.
[22] Unnikrishnan G, Thomas S. J Polym Sci B: Polym Phys 1997;35:725.
[23] Mathew AP, Pakirisamy S, Kumaran MG, Thomas S. Polymer 1995;36(26):4935.
[24] Johnson T, Thomas S. J Macromol Sci Phys 1997;B36(3):401.
[25] Mathai AE, Thomas S. J Macromol Sci Phys 1996;B35(2):229.
[26] George SC, Thomas S, Ninan KN. Polymer 1996;37(26):5839.
[27] Aminabhavi TM, Aithan US, Shukla SS. JMS Rev Macromol Chem Phys 1989;C29(2/3):319.
[28] Lawandy SN, Botros SH. J Appl Polym Sci 1991;42:137.
[29] Horkay F, Zrinyi M, Geissler E, Hecht AM, Pruvost P. Polymer 1991;32:835.
[30] Unnikrishnan G, Thomas S, Varghese S. Polymer 1996;37(13):2687.
[31] Hopfenberg HB, Paul DR. In: Paul DR, editor. Polymer blends, I. New York, NY: Academic Press, 1976.
[32] Kolarik J, Gueskens G. Polym Networks Blends 1997;7(1):13.
[33] Aminabhavi TM, Phayde HTS. J Appl Polym Sci 1995;55:1335.
[34] Asaletha R, Kumaran MG, Thomas S. Submitted to Polymer for publication.
[35] Robeson LM, Noshay A, Matzner M, Merriam CN. Die Angew Makromol Chem 1973;29/30:47.
[36] Flory PJ. Principles of polymer chemistry, Ithaca, NY: Cornell University Press, 1953.
[37] Mathew G, Singh RP, Lakshminarayan R, Thomas S. J Appl Polym Sci 1996;61:2035.